Chem. Chem. Technol., 2024,
Vol. 18, No. 3, pp. 313–320

Chemistry

SYNTHESIS, STRUCTURE AND ELECTROPHYSICAL PROPERTIES OF FLUORIDE-CONDUCTING PHASES $Ba_{1-X}La_XSnF_{4+X}$

Oleh Lysenko[1,✉], Roman Pshenychnyi[2], Tamara Pavlenko[1], Serhii Vorobiov[3], Anatoliy Omelchuk[1]

https://doi.org/10.23939/chcht18.03.313

Abstract. It has been determined that the concentration interval for the existence of solid solutions of heterovalent substitution $Ba_{1-x}La_xSnF_{4+x}$, which are formed by the partial replacement of barium cations with lanthanum cations in the $BaSnF_4$ compound, is $0.0 < x \leq 0.12$. The obtained phases are isostructural $BaSnF_4$, have a crystal lattice of tetragonal syngony, corresponding to the P4/nmm space group. The change in the values of electrical conductivity and its activation energy is extreme, with a maximum for the composition with lanthanum cation content of 0.07 m.p. and is $3.08 \cdot 10^{-3}$ S/cm at 623 K and $5.69 \cdot 10^{-4}$ S/cm at 293 K, respectively. The electrochemical stability window of the synthesized phases is estimated by the potential range of –1.7 ÷ +1.7 V.

Keywords: synthesis, fluoride-conducting phases, solid substitution solutions, fluorides of tin, barium, lanthanum, electrical conductivity, impedance spectroscopy, voltametry.

1. Introduction

An urgent task of modern science and technology is the creation of new electrode and electrolyte materials for current sources of the next generation. Recent studies[1] demonstrate the prospects of using fluoride-conducting solid electrolytes. Fluoride-conducting phases with high unipolar conductivity in the temperature range close to room temperature make it possible to create fundamentally new chemical current sources with specific characteristics that exceed the known ones[2]. Functional materials based on fluoride-conducting phases are not only practically used in chemical current sources but also in sensors, ion-selective electrodes, *etc*.[2–4].Therefore, the synthesis and study of the electrophysical properties of fluoride-conducting phases to create new electrode and electrolyte materials based on them are not only of scientific but also of applied importance.

Solid fluoride-conducting electrolytes, isostructural $PbSnF_4$, due to the presence of a single stereochemically active pair of $5s^2$ electrons of the Sn^{2+} cation have a sufficiently high unipolar conductivity for fluorine anions at room temperature and a relatively high electrochemical stability window, which attracts them for use in solid-state fluoride current sources[5–8]. The compound $BaSnF_4$ is isostructural to $PbSnF_4$, its crystal lattice corresponds to tetragonal syngony with a layered arrangement of cations •••BaBaSnSnBaBa••• along the *c* axis of the unit cell[9]. Due to this cation configuration, the mobile fluorine anions are primarily located in the Ba–Sn and Sn–Sn structures of the solid electrolyte. Ba–Ba layers act as barriers to conductivity in polycrystalline material since the fluorine anions located there are almost immobile. Consequently, their migration in the electric field in polycrystalline samples of fluoride-conducting phases based on $BaSnF_4$ occurs due to their jump into the space between layers Ba–Sn[10]. Therefore, the conductive properties of these compounds are significantly influenced not only by the concentration of defects in the crystal lattice but also by their location in the anionic sublattice between layers of cations.

Ionic transport in such structures generally depends on the structural framework, the intrinsic mobility of the conductive ions and their thermal activation, the concentration of internal and/or external defects, and the influence of the crystalline field of the moving ions. Ion diffusion mechanisms are mainly based on Schottky and anti-Frenkel point defects, including the vacancy mechanism, the internode mechanism, and the internode substitution exchange mechanism[11].

Conductivity can be improved by purposefully changing the concentration of defects in the crystal lattice of fluoride-conducting phases based on the $BaSnF_4$ compound by introducing heterovalent substituents into its composition, which can affect the mobility of fluorine

[1] V.I. Vernadsky Institute of General and Inorganic Chemistry, NAS of Ukraine, 32–34, Acad. Palladina Ave., 03680 Kyiv, Ukraine
[2] Sumy State University, 2, Rymskogo-Korsakova Str., 40007 Sumy, Ukraine
[3] Institute of Physics, Faculty of Science, P.J. Šafárik University, Park Angelinum, 9, 04013, Košice, Slovakia
✉ *lysenkooleh34@gmail.com*

anions and electrical conductivity. Substitution of barium ions for different cations leads to the formation of various types of defects in the structure of the electrolyte, which leads to an increase in the conductive properties of non-stoichiometric phases.

It was demonstrated[12] that replacing a part of the barium cations with Ce^{3+} cations in the $BaSnF_4$ compound can significantly influence its electrical conductivity. Thus, the conductivity of the fluoride-conducting phase of the $Ba_{0.95}Ce_{0.05}SnF_{4.05}$ composition is almost 3.5 times higher than the conductivity of the $BaSnF_4$ at room temperature and is $5.2 \cdot 10^{-4}$ S/cm. Furthermore, this electrolyte shows a lower activation energy than $BaSnF_4$ (0.15 eV *vs*. 0.25 eV).

It was also found that the doping of $BaSnF_4$ with Nd^{3+} and Eu^{3+} ions up to 3–4 mol % leads to the formation of additional interstitial fluorine ions, which increases the conductivity of these non-stoichiometric phases[13–15]. A further increase in the amount of dopant leads to a decrease in the conductivity parameters of the solid electrolyte.

The conductivity of conductive phase fluorides isostructural to $BaSnF_4$ is affected not only by heterovalent but also by isovalent substitution. For example, the replacement of some barium cations with manganese cations in the original structure increases the conductivity. It was shown[16] that $Ba_{0.96}Mn_{0.04}SnF_{4.00}$ composition at room temperature has a conductivity of $2.7 \cdot 10^{-4}$ S/cm, which exceeds the conductivity of $BaSnF_4$.

The conductivity and structural features of the fluoride-conducting phases formed in the BaF_2-SnF_2 binary system were studied by several authors[7, 17, 18]. It was found[7] that the non-stoichiometric phase of $Ba_{0.47}Sn_{0.53}F_{4.00}$ composition has the highest electrical conductivity ($\sigma = 4.1 \cdot 10^{-3}$ S/cm at room temperature) and the lowest activation energy of ionic conductivity (Ea = 17.9 kJ/mol).

This work is aimed to study the effect of substitution of part of Ba^{2+} cations in the $BaSnF_4$ initial structure with a heterovalent substituent with a similar radius (La^{3+}) to discover new solid fluoride-conducting phases that can be of practical importance in the field of electrical engineering.

2. Experimental

2.1. Materials

To obtain solid solutions of the $Ba_{1-x}La_xSnF_{4+x}$ composition, reagents with a sufficient content of the main substance were used: Ba $(NO_3)_2$ (99.95 %), La_2O_3 (99 %), SnF_2 (99 %), and NH_4F (99 %).

2.2. Methods

2.2.1. Synthesis of Solid Solutions

$Ba_{1-x}La_xSnF_{4+x}$ solid solutions were synthesized in several stages[19–21]. At the first stage, solid solutions of the $Ba_{1-x}La_xF_{2+x}$ composition (x = 0.01; 0.03; 0.05; 0.07; 0.10; 0.12) were obtained by the coprecipitation method from the solutions. The investigated concentration interval was limited by the lanthanum content x = 0.12; above this value, it was impossible to obtain single-phase products by this method. Initially, a 0.1 M solution of $La(NO_3)_3$ was prepared by dissolving the calculated amount of lanthanum oxide in concentrated nitrate acid, followed by dilution with distilled water. A 0.1 M solution of $Ba(NO_3)_2$ was prepared by dissolving the salt in distilled water. Then the two solutions were mixed in the appropriate ratio, stirred for 10 min on a magnetic stirrer, and added dropwise to a sevenfold excess of NH_4F solution to complete the co-precipitation of barium and lanthanum fluorides. The resulting precipitate was separated from the residues of soluble cations and anions in a centrifuge by washing with distilled water. Then it was dried at 333 K in an oven for 48 h.

At the second stage, the resulting solid solutions were mixed with an equivalent amount of SnF_2, crushed and homogenized in an agate mortar, and the mixture was pressed into tablet samples under a pressure of 7 MPa, which were subsequently sintered to obtain non-stoichiometric phases of the $Ba_{1-x}La_xSnF_{4+x}$ composition. The synthesis was carried out at a temperature of 773 K for 30 min in an argon atmosphere to prevent the formation of oxides and oxyfluorides.

2.2.2. X-ray Diffraction Analysis

X-ray diffraction analysis (XRD) of the synthesized samples was performed on a DRON-3M diffractometer with CuK_α radiation in the range of angles from 10 to 80 deg. with a step of 0.04 deg. and an exposure of 3 s at each point. The JCPDS database was used to identify the diffractograms. Processing of diffraction patterns and calculations of unit cell volumes were carried out using the computer programs Match and UnitCell.

2.2.3. Energy Dispersive X-ray Spectroscopy

The chemical composition of $Ba_{1-x}La_xSnF_{4+x}$ solid solutions was determined using a Tescan Vega scanning electron microscope equipped with an energy dispersive X-ray detector (Oxford detector). For each sample, three measurements were taken from different areas, subsequently averaged to obtain reliable results. The measurement error was up to 3 %.

2.2.4. Alternating Current Bridge Method

The electrical conductivity of the synthesized samples was studied by the alternating current method

using a two-electrode circuit with the help of an alternating current bridge P5083. Cylindrical polycrystalline samples with a diameter of 8.0 mm and a thickness of 1.3–1.6 mm pressed under a pressure of 10 MPa for 3 min were used for the research. The current leads to the samples were polished platinum plates.

The temperature dependence of the electrical conductivity of complex fluorides was studied at a frequency of 100 kHz. Measurements were carried out in an argon atmosphere at 298–623 K after thermostating in the cooling mode. The temperature measurement error was up to 1 %, and the electrical conductivity was up to 4 %.

The specific electrical conductivity was calculated according to Eq. (1)

$$\sigma = l/s \cdot R, \quad (1)$$

where l is the thickness of the cylindrical sample, s is the contact area, and R is the active resistance.

2.2.5. Impedance Spectroscopy

Impedance was measured using a broadband dielectric spectrometer RLC E7-30. The pressed (10 MPa for 3 min) cylindrical polycrystalline samples with a diameter of 8 mm and thickness of 1.6 mm were placed between two polished platinum electrodes in the sample cell, which was then heated to operating temperature. After thermostating the sample in the cooling mode, measurements were made in the frequency range from 25 Hz to 3 MHz at the temperature range from room to 523 K. The measurement error was up to 3 %. The electrohemical impedance spectrum of the solid electrolyte was modeled using the EIS Spectrum Analyzer software.

2.2.6. Cyclic Voltammetry

Studies of the electrochemical stability window were performed by cyclic voltammetry using the MTech POL-21 device in a two-electrode cell with platinum electrodes at potential scanning rates of 10 mV/s at a temperature of 373 K. Cylindrical polycrystalline samples with a diameter of 8.0 mm and a thickness of 2.0–3.0 mm pressed under a pressure of 10 MPa for 3 min were used for the research.

3. Results and Discussion

3.1. Study on the Phase Composition of the Obtained Phases of the $Ba_{1-x}La_xF_{2+x}$ Composition

According to the results of XRD analysis, solid solutions of the $Ba_{1-x}La_xF_{2+x}$ composition have a cubic crystal lattice (sp. group Fm^3m) and are isostructural to BaF_2 (JCPDS card No. 00-004-0452) (Fig. 1, *a*). The volume of unit cells of the synthesized samples linearly decreases with an increase in the substituent content (Fig. 1, *b*), which corresponds to the rules of crystallographic substitution. The effective ionic radii of cations Ba^{2+} and La^{3+} are 0.135 and 0.101 nm, respectively (for VI coordination)[22]. Unit cell volumes decrease from 2.387 nm^3 for BaF_2 to 2.382 nm^3 for $Ba_{0.88}La_{0.12}F_{2.12}$. It is noted that the second phase of isostructural BaF_2 is formed in the synthesized samples with a substituent content of $x \geq 0.10$, but with a shorter lattice period than that of the main solid solution. The diffractograms of the samples with substituent content $x = 0.10$ and 0.12 (Fig. 1, *a*) clearly show additional reflexes of the first four diffraction reflexes of the main phase maxima.

3.2. Study on the Synthesis Conditions of Solid Solutions of the $Ba_{1-x}La_xSnF_{4+x}$ Composition

The optimal conditions for the synthesis of non-stoichiometric phases of $Ba_{1-x}La_xSnF_{4+x}$ were determined by studying the dependence of X-ray diffractograms on the duration and sintering temperature of the solid solution of $Ba_{1-x}La_xF_{2+x}$ and SnF_2. The optimal sintering time was determined as follows: samples prepared under the same conditions were sintered at 773 K in an argon atmosphere with different holding times. According to the XRD data (Fig. 2, *a*), the sample synthesized for 30 min has the highest quality crystal structure, and the sample with a holding time of 40 min already shows the formation of impurity phase signals. The impurity phase can be attributed to the formation of tin (IV) oxide (JCPDS card No. 00-001-0625). At the next stage, the prepared samples were sintered for 30 min at different temperatures from 623 K to 823 K.

It was found that the resulting structure (P4/nmm) was formed in the entire temperature range studied (Fig. 2, *b*). To prevent the loss of tin (II) fluoride during synthesis and to ensure a more uniform distribution of the substituent in the sample volume, sintering was performed at 773 K.

3.3. Determination of the Phase Composition of the $Ba_{1-x}La_xSnF_{4+x}$ Synthesized Samples

$Ba_{1-x}La_xSnF_{4+x}$, which was obtained at the second stage of the synthesis phase, has a tetragonal crystal lattice (P4/nmm) and is isostructural to $BaSnF_4$ (JCPDS card No. 00-038-0738) (Fig. 3). The maximum content of x substituent (La^{3+}) in the resulting phases is 0.12. Calculation of unit cell volumes showed that substitution of a part of Ba^{2+} cations with La^{3+} cations does not significantly affect the unit cell volume of the $Ba_{1-x}La_xSnF_{4+x}$ obtained phases.

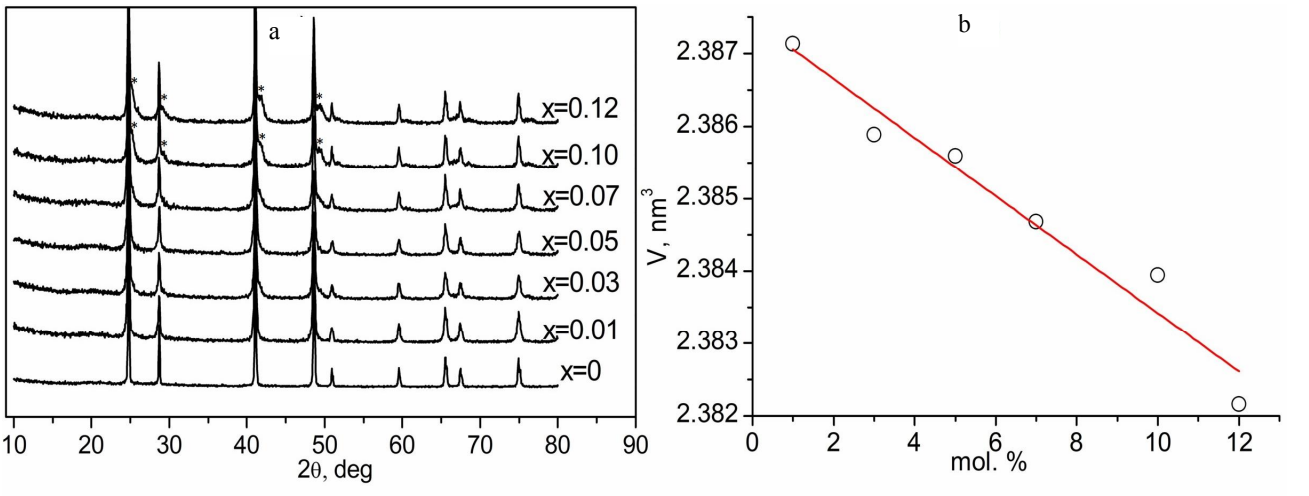

Fig. 1. Diffraction patterns (a) and unit cell volumes (b) of solid solutions of $Ba_{1-x}La_xF_{2+x}$

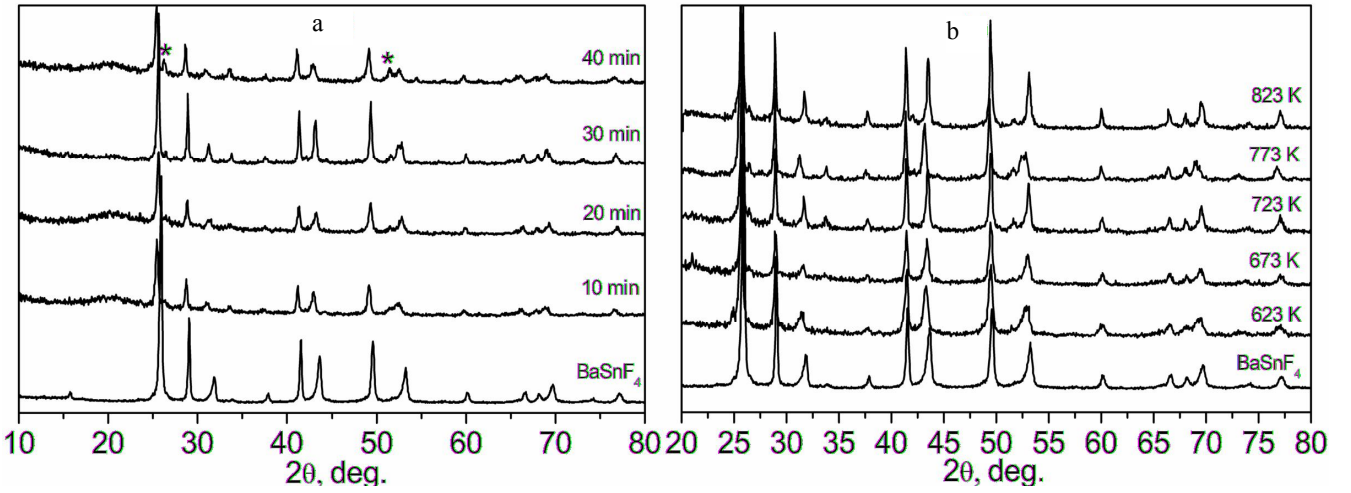

Fig. 2. $Ba_{0.95}La_{0.05}SnF_{4.05}$ diffractograms: dependence on the synthesis duration (a) and dependence on the synthesis temperature (b)

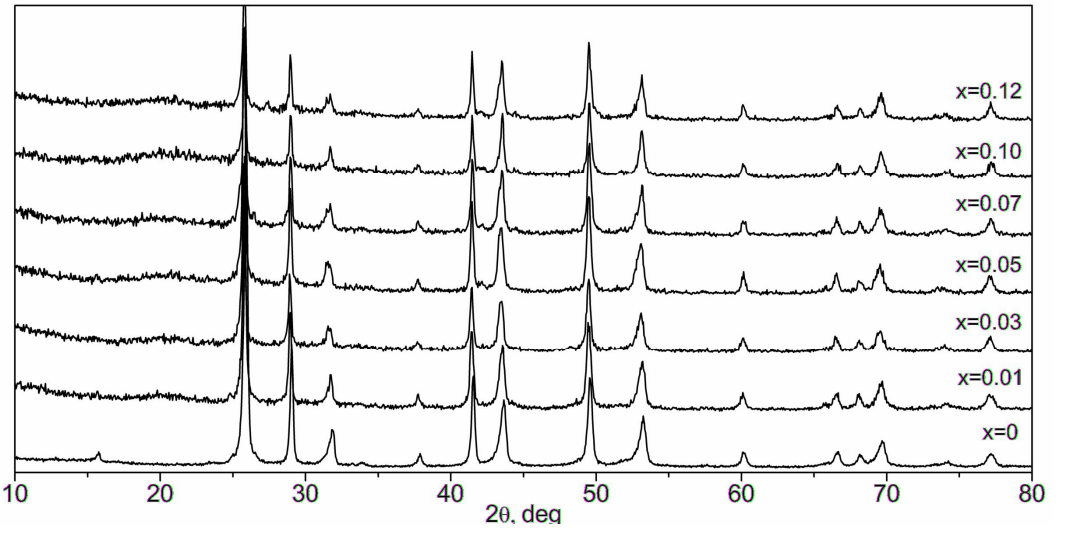

Fig. 3. Diffractograms of $Ba_{1-x}La_xSnF_{4+x}$ solid solutions

Table 1. Elemental composition of $Ba_{1-x}La_xSnF_{4+x}$ solid solutions

Calculated mixture composition			EDX results after synthesis	
Formula	Element	at %	at %	Composition, mole
$BaSnF_4$	Ba	16.66	16.49	0.99
	Sn	16.67	16.84	1.01
	F	66.67	66.67	4.00
$Ba_{0.99}La_{0.01}SnF_{4.01}$	Ba	16.47	16.61	1.00
	La	0.17	0.17	0.01
	Sn	16.64	16.45	0.99
	F	66.72	66.77	4.02
$Ba_{0.97}La_{0.03}SnF_{4.03}$	Ba	16.09	16.39	0.99
	La	0.50	0.53	0.03
	Sn	16.58	16.22	0.98
	F	66.83	66.86	4.04
$Ba_{0.95}La_{0.05}SnF_{4.05}$	Ba	15.70	15.83	0.96
	La	0.83	0.81	0.05
	Sn	16.53	16.31	0.99
	F	66.94	67.05	4.07
$Ba_{0.93}La_{0.07}SnF_{4.07}$	Ba	15.32	15.49	0.94
	La	1.15	1.22	0.07
	Sn	16.48	16.07	0.98
	F	67.05	67.22	4.08
$Ba_{0.90}La_{0.10}SnF_{4.10}$	Ba	14.75	14.91	0.91
	La	1.64	1.81	0.11
	Sn	16.39	15.89	0.97
	F	67.21	67.39	4.11
$Ba_{0.88}La_{0.12}SnF_{4.12}$	Ba	14.19	14.17	0.87
	La	2.12	2.20	0.13
	Sn	16.31	16.24	1.00
	F	67.37	67.39	4.14

3.4. Determination of the Chemical Composition of the Obtained $Ba_{1-x}La_xSnF_{4+x}$ Solid Solutions

Based on the results of energy dispersive analysis for the obtained solid solutions, it was determined that the elemental composition of the resulting materials is almost identical to the calculated values (see Table 1). Minor deviations from the composition of the formula noted in the analysis results may be due to the evaporation of SnF_2 and instrument error.

3.5. Ionic Conductivity Test of the Synthesized Samples of $Ba_{1-x}La_xSnF_{4+x}$ Solid Solutions

Analysis of the conductivity isotherms of the synthesized samples of non-stoichiometric phases $Ba_{1-x}La_xSnF_{4+x}$ showed that an increase in the substituent content to $x = 0.07$ increases the conductivity (Fig. 4, *b*). This may be due to the substitution of part of the nodal barium cations with lanthanum cations, increasing the concentration of interstitial fluorine anions F_i':

$$LaF_3\left(BaF_3\right) \rightarrow La^*_{Ba} + F_i' \quad (2)$$

The substitution scheme is given according to the Kröger-Vink notation.

As a result, with an increase in the lanthanum content in the solid solution sample, the concentration of mobile interstitial fluorine anions F_i' increases, which is responsible for the conductivity of the following phases[15–17]. The best conductivity values have the $Ba_{0.93}La_{0.07}SnF_{4.07}$ phase, for which $\sigma = 1.53 \cdot 10^{-3}$ S/cm at 353 K.

Analysis of temperature dependencies of electric conductivity of the synthesized samples of fluoride-conducting phases makes it possible to distinguish two straight sections in high-temperature and low-temperature regions. Both are satisfactorily approximated by the Arrhenius – Frenkel equation (3), as evidenced by the calculated values of the determination coefficient R^2 (Table 2):

$$\sigma T = A\exp(-\Delta E_a / kT), \quad (3)$$

where σT product of specific electrical conductivity by temperature expressed in Kelvin degrees, A is the pre-exponential factor, ΔE_a is the activation energy of ion conductivity, and k is the Boltzmann constant.

The presence of this effect may be due to structural changes in the solid electrolyte, due to which the amount of fluorine anions in the interstitial spaces of the crystal lattice increases as a result of heating the solid electrolyte[19, 23]. Fluoride ions in the leading phases with fluorite and tysonite structure occupy three different positions[7, 24], differing from each other by cationic environment and bond length M–F. At a certain temperature, locally mobile fluoride anions acquire energy sufficient to overcome the energy barrier and pass into the internode space. With a further increase in temperature, the concentration of charge carriers practically does not change but only their mobility increases.

The calculated values of the activation energy of ionic conductivity of the obtained solid solutions are lower than those of the original $BaSnF_4$ compound, and this pattern is observed over the entire temperature range under study (Table 2). This may be due to the effect of the heterovalent substituent on the structure of the solid electrolyte. The values of the activation energy of ionic conductivity gradually decrease with an increase in the substituent content up to $x = 0.07$, then these values gradually increase. The $Ba_{0.93}La_{0.07}SnF_{4.07}$ phase is characterized by the lowest values of the activation energy of ionic conductivity and is 0.237 eV in the high-temperature region and 0.085 eV in the low-temperature region.

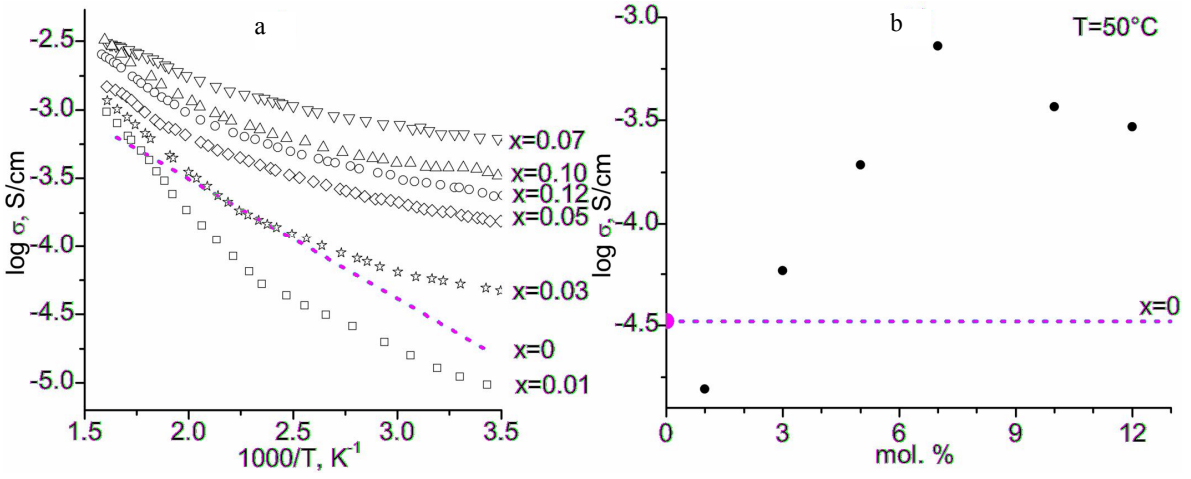

Fig. 4. Electrical conductivity of the synthesized samples of polycrystalline fluoride-conducting phases $Ba_{1-x}La_xSnF_{4+x}$ at different temperatures and substituent content (a) and electrical conductivity isotherm at 353 K (b)

Table 2. Parameters of electrical conductivity of $Ba_{1-x}La_xSnF_{4+x}$ solid solutions

Sample		ΔE_a, eV ± 0.01	lg(A), (S/cm)·K	σ, S/cm ± 4%	T, K ± 2	R^2
$Ba_{0.99}La_{0.01}SnF_{4.01}$	622–425	0.386	2.89	$9.62\cdot10^{-4}$	622	0.9964
	425–291	0.167	0.31	$9.71\cdot10^{-6}$	291	0.9967
$Ba_{0.97}La_{0.03}SnF_{4.03}$	621–413	0.284	2.14	$1.21\cdot10^{-3}$	621	0.9947
	413–286	0.115	0.12	$4.71\cdot10^{-5}$	286	0.9767
$Ba_{0.95}La_{0.05}SnF_{4.05}$	625–445	0.224	1.74	$1.48\cdot10^{-3}$	625	0.9837
	445–286	0.101	0.39	$1.55\cdot10^{-4}$	286	0.9884
$Ba_{0.93}La_{0.07}SnF_{4.07}$	623–480	0.172	1.69	$3.08\cdot10^{-3}$	622	0.9955
	480–291	0.086	0.73	$5.69\cdot10^{-4}$	285	0.9948
$Ba_{0.90}La_{0.10}SnF_{4.10}$	626–435	0.237	2.18	$3.25\cdot10^{-3}$	626	0.9906
	435–287	0.085	0.46	$3.31\cdot10^{-4}$	287	0.9745
$Ba_{0.88}La_{0.12}SnF_{4.12}$	631–441	0.236	2.07	$2.54\cdot10^{-3}$	631	0.9912
	441–284	0.098	0.53	$2.38\cdot10^{-4}$	284	0.9899

The typical nature of the impedance hodographs of all tested samples of solid solutions of this system in the complex plane Z'–Z" on the example of the $Ba_{0.93}La_{0.07}SnF_{4.07}$ composition is given in Fig. 5. With increasing temperature, the impedance of all tested samples decreases, which indicates an increase in ion conductivity during heating. The obtained spectra are satisfactorily approximated by the equivalent scheme provided in the insert (left, top, Fig. 5). The resulting dependence can be approximated by an equivalent circuit in which a constant phase element (CPE) and volume resistivity R are connected in parallel[25]. The conductivity

data calculated from the impedance spectra are in good agreement with the values obtained by the alternating current method.

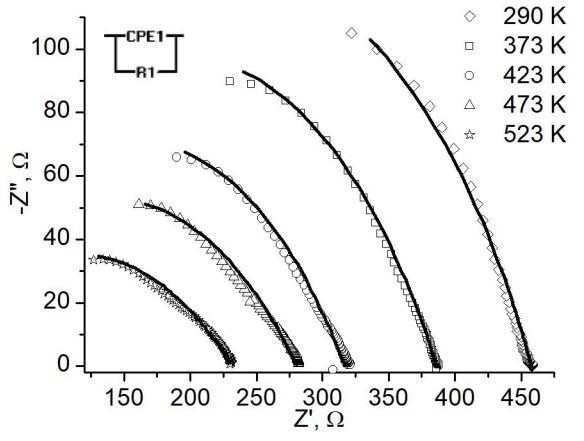

Fig. 5. Impedance spectra of $Ba_{0.93}La_{0.07}SnF_{4.07}$ at different temperatures

3.6. Voltammetric Studies of the Synthesized Samples of $Ba_{1-x}La_xSnF_{4+x}$ Solid Solutions

The typical character of the voltammograms of the synthesized samples of $Ba_{1-x}La_xSnF_{4+x}$ solid solutions is presented on the example of voltammogram of the $Ba_{0.95}La_{0.05}SnF_{4.05}$ sample. At potentials above –1.7 V in the cathode region, both during the forward and reverse potential scan, an increase in the current flowing through the cell is recorded. In the anode region, at potentials of +1.7 V, an increase in the current flowing through the cell is also recorded, both during the forward and reverse potential sweep (Fig. 6, *a*). This gives reason to believe that in the interval of +1.7 V ÷ –1.7 V, almost no electrochemical transformations occur in the synthesized sample. It was noted that when the voltammetry cycles in the potential range below its decomposition potential, the character of the voltammetry practically does not change (Fig. 6, *b*).

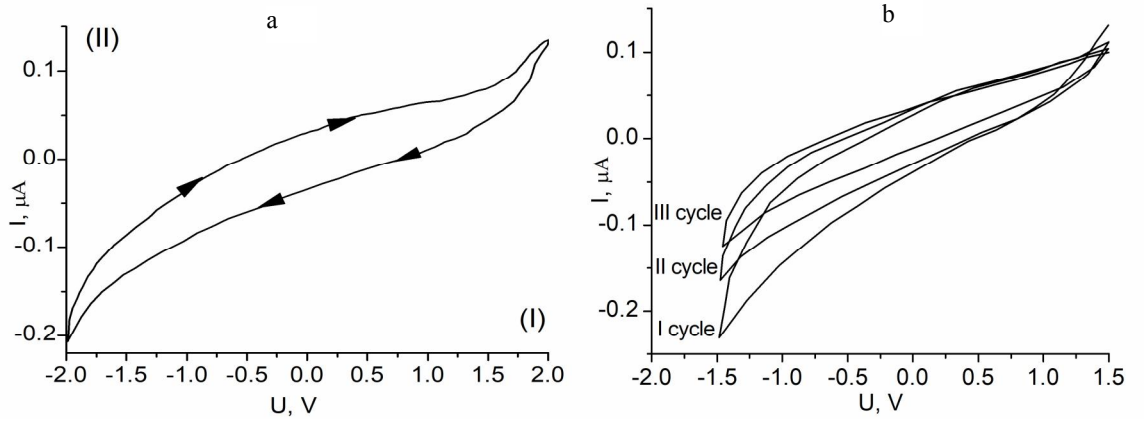

Fig. 6. Cyclic voltammograms of $Ba_{0.95}La_{0.05}SnF_{4.05}$ at T = 373 K and a sweep speed of 10 mV/s: value of ESW (a) and electrochemical behavior during 3 cycles (b)

4. Conclusions

Single-phase fluorine-conducting solid solutions of heterovalent substitution $Ba_{1-x}La_xSnF_{4+x}$ with an isostructural lattice of $BaSnF_4$ corresponding to tetragonal syngonality (P4/nmm) were obtained. The concentration interval of fluoride formation in the conductive phases of the $Ba_{1-x}La_xSnF_{4+x}$ composition was determined, which is 0.12 m.p. of lanthanum content.

It was established that with an increase in the substituent content in the synthesized phases to $x \leq 0.07$, their electrical conductivity increases, and the activation energy decreases. With a further increase in the substituent content, the electrical conductivity decreases, and its activation energy increases. The $Ba_{0.93}La_{0.07}SnF_{4.07}$ sample has the highest electrical conductivity of $3.08 \cdot 10^{-3}$ S/cm at 623 K and $5.69 \cdot 10^{-4}$ S/cm at 293 K.

It was demonstrated that the introduction of a substituent reduced the activation energy for all samples compared to the parent compound. Phase containing 0.07 m.p. La^{3+} is characterized by the lowest values of ion conductivity activation energy, which is 0.172 eV in the high-temperature region and 0.086 eV in the low-temperature region.

It was found that in the potential range of + 1.7 V ÷ – 1.7 V, the synthesized samples of fluorine-conducting phases practically do not undergo electrochemical transformations, which indicates the possibility of their use in this potential range as electrolyte materials for solid-state electrophysical devices

References

[1] Sandstrom, SK.; Chen, X.; Ji, X. A Review of Halide Charge Carriers for Rocking-Chair and Dual-Ion Batteries. *Carbon Energy* **2021**, *4*, 627–653. https://doi.org/10.1002/cey2.110

[2] Nowroozi, J. M.; Mohammad, I.; Molaiyan, P.; Wissel, K.; Reddy, M. A.; Clemens O. Fluoride Ion Batteries – Past, Present, and Future. *J. Mater. Chem. A* **2021**, *9*, 5980–6012. https://doi.org/10.1039/D0TA11656D

[3] Kumaravel, V.; Bartlett, J.; Pillai, S.C. Solid Electrolytes for High-Temperature Stable Batteries and Supercapacitors. *Adv. Energy Mater.* **2020**, *11*, 1–42. https://doi.org/10.1002/aenm.202002869

[4] Liu, T.; Peng, N.; Zhang, X.; Zheng, R.; Xia, M.; Zhang, J.; Yu, H.; Zhang, L.; Shu, J. Insight into Anion Storage Batteries: Materials, Properties and Challenges. *Energy Stor. Mater.* **2021**, *42*, 42–67. https://doi.org/10.1016/j.ensm.2021.07.011

[5] Patro, L.N.; Hariharan, K. Fast Fluoride Ion Conducting Materials in Solid State Ionics: An Overview. *Solid State Ion.* **2013**, *239*, 41–49. https://doi.org/10.1016/j.ssi.2013.03.009

[6] Mohammad, I.; Witter, R.; Fichtner, M.; Reddy, M. A. Introducing Interlayer Electrolytes: Toward Room-Temperature High-Potential Solid-State Rechargeable Fluoride Ion Batteries. *ACS Appl. Energy Mater.* **2019**, *2*, 1553–1562. https://doi:10.1021/acsaem.8b02166

[7] Mori, K.; Mineshige, A.; Emoto, T.; Sugiura, M.; Saito, T.; Namba, K.; Otomo, T.; Abe, T.; Fukunaga, T. Electrochemical, Thermal, and Structural Features of BaF_2–SnF_2 Fluoride-Ion Electrolytes. *J. Phys. Chem. C* **2021**, *125*, 12568–12577. https://doi:10.1021/acs.jpcc.1c03326

[8] Dénès, G.; Hantash, J.; Muntasar, A.; Oldfier, P. Variations of $BaSnF_4$ Fast Ion Conductor with the Method of Preparation and Temperature. *Hyp. Int.* **2006**, *170*, 145–158. https://doi:10.1007/s10751-006-9464-5

[9] Chaudhuri, S.; Wang, F.; Grey, C.P. Resolving the Different Dynamics of the Fluorine Sublattices in the Anionic Conductor $BaSnF_4$ by Using High-Resolution MAS NMR Techniques. *J. Am. Chem. Soc.* **2002**, *124*, 11746–11757. https://doi.org/10.1021/ja026155j

[10] Liu, L.; Yang, L.; Liu, M.; Li, X.; Shao, D.; Luo, K.; Wang, X.; Luo, Z. SnF_2-Based Fluoride Ion Electrolytes $MSnF_4$ (M = Ba, Pb) for the Application of Room-Temperature Solid-State Fluoride Ion Batteries. *J. Alloys Compd.* **2020**, *819*, 152983–153013. https://doi:10.1016/j.jallcom.2019.152983

[11] Dudney, N.J.; West, W.C., Nanda, J. *Materials and Energy* - Vol. 6. Handbook of Solid State Batteries, 2nd ed.; World Scientific, 2015. https://doi.org/10.1142/9487

[12] Liu, J.; Yi, L.; Zeng, P.; Zou, C.; Chen, X.; Tao, X.; Liu, X.; Yang, L.; Zang, Z.; Chang, B.; *et al*. Point Defect Engineering Enabled the High Ionic Conductivity of $BaSnF_4$ for Solid-State Fluoride-Ion Batteries at Room Temperature. *Energy Fuels* **2022**, *36*, 15258–15267. https://doi.org/10.1021/acs.energyfuels.2c03509

[13] Patro, L.N.; Hariharan, K. Rare Earth Ions (Eu^{3+} and Nd^{3+}) Doped $BaSnF_4$: Transport and Photoluminescence Characteristics. *Ionics* **2013**, *19*, 1611–1617. https://doi.org/10.1007/s11581-013-0896-z

[14] Liu, L.; Yang, L.; Shao, D.; Zou, C.; Luo, Z.; Wang, X. Nd^{3+} Doped $BaSnF_4$ Solid Electrolyte for Advanced Room-Temperature Solid-State Fluoride Ion Batteries. *Ceram. Int.* **2020**, *46*, 20521–20528. https://doi:10.1016/j.ceramint.2020.05.16

[15] Zang, Z.; Liu, L.; Yang, L.; Luo, K.; Zou, C.; Chen, X.; Tao, X.; Luo, Z.; Chang, B.; Wang, X. Preparation and Performance of Eu^{3+}-Doped $BaSnF_4$-Based Solid-State Electrolytes for Room-Temperature Fluoride-Ion Batteries. *ACS Sustainable Chem. Eng.* **2021**, *9*, 12978–12989. https://doi.org/10.1021/acssuschemeng.1c04523

[16] Zang, Z.; Liu, J.; Tao, X.; Zou, C.; Chen, X.; Yi, L.; Chang, B.; Wang, X. Mn^{2+} Doped $BaSnF_4$-Based Solid State Electrolyte for Room-Temperature Fluoride Ion Batteries. *J. Electroanal. Chem.* **2023**, *930*, 117145. https://doi.org/10.1016/j.jelechem.2023.117145

[17] Ahmad, M.M.; Yamane, Y.; Yamada, K. The Ionic Conductivity and Dielectric Properties of $Ba_{1-x}Sn_xF_2$ Solid Solutions Prepared by Mechanochemical Milling. *Mater. Sci. Eng.: B.* **2013**, *178*, 965–970. https://doi.org/10.1016/j.mseb.2013.05.011

[18] Pshenichny, R.N.; Pogorenko, Y.V.; Pavlenko, T.V.; Omelchuk, A.O. Synthesis, Structure and Properties of Solid Solutions $Ba_{1-x}Sn_{1+x}F_4$ і $(K_yBa_{1-y})_{(1-x)}Sn_{1+x}F_{4-y(1-x)}$. *Vopr. Khimii i Khimicheskoi Tekhnologii* **2021**, *1*, 62–70. https://doi.org/10.32434/0321-4095-2021-134-1-62-70

[19] Pogorenko, Y.V.; Pshenychnyi, R.M.; Omelchuk, A.O.; Trachevskyi, V.V. Conductivity of Aliovalent Substitution Solid Solutions $Pb_{1-x}R_xSnF_{4+x}$. *Solid State Ion.* **2019**, *338*, 80–86. https://doi.org/10.1016/j.ssi.2019.05.001

[20] Pogorenko, Y.V.; Pshenychnyi, R.M.; Lutsyk, V.I.; Omelchuk, A.O. Transport Properties of Aliovalent Substitution Solid Solutions of the System (1-x)$PbF_{2-x}YF_3$-SnF_2. *IOP Conf. Ser.: Mater. Sci. Eng.* **2017**, *175*, 012039. https://doi.org/10.1088/1757-899X/175/1/012039

[21] Pshenichny, R.N.; Lysenko, O.V.; Pavlenko, T.V.; Omelchuk, A.O. Conductive Properties of Solid Solutions of the System xYF_3-(1-x)BaF_2-SnF_2. *Funct. Mater.* **2023**, *30*, 18–23. https://doi.org/10.15407/fm30.01.18

[22] Shannon, R.D. Revised Effective Ionic Radii and Systematic Studies of Interatomic Distances in Halides and Chalcogenides. *Acta Cryst.* **1976**, *32*, 751–767. https://doi.org/10.1107/S0567739476001551

[23] Yoshikado, Sh.; Ito, Y.; Réau, J.M.; Fluoride ion Conduction in $Pb_{1-x}Sn_xF_2$ Solid Solution System. *Solid State Ion.* **2002**, *503*, 154–155. https://doi.org/10.1016/S0167-2738(02)00489-7

[24] Martineau, C.; Fayon, F.; Legein, C.; Buzare, J-Y.; Corbel, G. Solid-State ^{19}F MAS NMR Investigation of Fluoride Ion Mobility in Lead Fluorides: Correlation with Anionic Conductivity. *Chem. Mater.* **2010**, *22*, 1585–1594. https://doi.org/10.1021/cm9030182

[25] Wortmann, M.; Frese, N.; Mamun, A.; Trabelsi, M.; Keil, W.; Buker, B.; Javed, A.; Tiemann, M.; Moritzer, E.; Ehrmann, A.; *et al*. Chemical and Morphological Transition of Poly(acrylonitrile)/Poly(vinylidene Fluoride) Blend Nanofibers during Oxidative Stabilization and Incipient Carbonization. *Nanomaterials* **2020**, *10*, 1210–1230. https://doi.org/10.3390/nano10061210

Received: December 18, 2023 / Revised: February 15, 2024 / Accepted: February 28, 2024

СИНТЕЗ ТА ЕЛЕКТРОФІЗИЧНІ ВЛАСТИВОСТІ ФТОРИДПРОВІДНИХ ФАЗ $Ba_{1-x}La_XSnF_{4+x}$

Анотація. *Встановлено, що концентраційний інтервал існування твердих розчинів гетеровалентного заміщення $Ba_{1-x}La_xSnF_{4+x}$, утворених за часткової заміни катіонів барію катіонами лантану в сполуці $BaSnF_4$, становить $0,0<x\leq0,12$. Утворені фази ізоструктурні $BaSnF_4$ мають кристалічну ґратку тетрагональної сингонії, яка відповідає просторовій групі P4/nmm. Зміна значень електропровідності й енергії її активації є екстремальною з максимумом для складу із вмістом катіонів лантану 0,07 м.ч. і становить $3,08\cdot10^{-3}$ См/см за 623 К і $5,69\cdot10^{-4}$ См/см за 293 К. Вікно електрохімічної стійкості синтезованих фаз оцінюється інтервалом потенціалів –1,7 ÷ +1,7 В.*

Ключові слова: *синтез, фторидпровідні фази, тверді розчини заміщення, фториди стануму, барію, лантану, електропровідність, імпедансна спектроскопія, циклічна вольтамперометрія.*